0026-895X/90/060785-12$03.00/0

MOLECULAR PHARMACOLOGY, 38:785-796

Bradykinin-Induced Modulation of Calcium Signals in Rat Dorsal Root Ganglion Neurons *In Vitro*

DAVID BLEAKMAN, STANLEY A. THAYER,[1] STEVEN R. GLAUM, and RICHARD J. MILLER
Department of Pharmacological and Physiological Sciences, University of Chicago, Chicago, Illinois 60637
Received January 12, 1990; Accepted August 27, 1990

SUMMARY

We used combined patch-clamp-microfluorimetric recordings to examine the effects of bradykinin on $[Ca^{2+}]_i$ transients and the Ca^{2+} current (I_{Ca}) in rat dorsal root ganglion neurons *in vitro*. Bradykinin increased $[Ca^{2+}]_i$ in approximately 20% of dorsal root ganglion cells examined and inhibited the I_{Ca} in approximately 65% of dorsal root ganglion cells. Bradykinin also inhibited the I_{Ca} when $[Ca^{2+}]_i$ was buffered with 1,2-bis(2-aminophenoxy)ethane-*N*,*N*,*N'*,*N'*-tetraacetic acid or when Ba^{2+} was the charge carrier. When I_{Ca}'s of increasing duration were elicited in these neurons, $[Ca^{2+}]_i$ transients were produced that increased in amplitude but eventually approached an asymptote at longer voltage steps. Similarly, the amplitude of the $[Ca^{2+}]_i$ transient also approached an asymptote in current-clamp recordings when cells were induced to fire a large number of action potentials. The bradykinin-induced inhibition of the amplitude of the $[Ca^{2+}]_i$ transient was more pronounced at shorter voltage steps. At pulse durations that produced asymptotic $[Ca^{2+}]_i$ signals, bradykinin no longer decreased the amplitude of the rise in $[Ca^{2+}]_i$, although it still reduced the I_{Ca}. In current-clamp recordings, bradykinin also reduced the $[Ca^{2+}]_i$ signal that accompanied the generation of action potentials, but again bradykinin was more effective for shorter spike trains. Bradykinin also depolarized the majority of neurons (65%). The reduction in $[Ca^{2+}]_i$ produced by bradykinin in sensory neurons may be an important factor contributing to bradykinin-induced excitation of primary sensory afferents.

BK is a nonapeptide that plays a central role in the production of pain and inflammation. BK has been shown to stimulate the transmission of nociceptive information from the periphery into the central nervous system (1). In particular, BK has been shown to activate both cutaneous nociceptive afferents and afferents from muscle (2). However, the molecular mechanisms through which BK produces neuronal excitation have remained elusive. Several reports have identified BK-induced effects on both sensory neurons and neuronal cell lines (reviewed in Ref. 3). BK has been reported to inhibit a Ca^{2+}-activated K^+ current, $I_{K(Ca)}$ (4), and a Ca^{2+} current, I_{Ca} (5), in sensory neurons as well as to produce a Na^+-dependent diacylglycerol-mediated depolarization of these cells (6–8). The situation is complicated by the fact that various different populations of sensory neurons exist that can be categorized either functionally (9), anatomically (10), or histologically (11, 12), several of which may be modulated by BK. Several of the important effects produced by BK (e.g., inositol trisphosphate synthesis or inhibition of the I_{Ca}) may result in changes in the neuronal $[Ca^{2+}]_i$, which could then play a key role in the subsequent regulation of neuronal excitability and the release of neurotransmitters in the spinal cord. It is possible that the different effects produced by BK may be present in different subpopulations of sensory neurons, but whether this is so is generally unclear. It is also unclear at present whether the BK-dependent inhibition of the I_{Ca} is secondary to the observed increase in $[Ca^{2+}]_i$ produced by BK.

In the present series of experiments, we have used simultaneous electrophysiological-microfluorimetric recordings of sensory neurons *in vitro* to examine some of the ways in which BK modulates $[Ca^{2+}]_i$ in these cells. The results demonstrate that BK regulation of $[Ca^{2+}]_i$ in these neurons depends critically upon the activation state of the cell and also suggest a mechanism that could partly explain how BK normally regulates sensory neuron excitability.

Materials and Methods

Instrumentation. The methods used for this study have been described previously in detail (13). Briefly, for excitation of the fluorescent calcium probe fura-2 (pentapotassium salt), the collimated

This work was supported by United States Public Health Service Grants DA-02575, DA-02121, and MH-40165 and grants from Miles Laboratories and Marion Laboratories to R.J.M. and senior fellowships from the Chicago Heart Association to D.B. and S.A.T. D.B. was also supported by a Fulbright Travel Fellowship. S.R.G. was supported by National Institutes of Health Grant T32HL7237-14.
[1] Current address: Department of Pharmacology, University of Minnesota, 435 Delaware St. S.E., Minneapolis, MN 55455.

ABBREVIATIONS: BK, bradykinin; DRG, dorsal root ganglion; HEPES, 4-(2-hydroxyethyl)-1-piperazineethanesulfonic acid; EGTA, ethylene glycerol bis(β-aminoethyl)-*N*,*N*,*N'*,*N'*-tetraacetic acid; BAPTA, 1,2-bis(2-aminophenoxy)ethane-*N*,*N*,*N'*,*N'*-tetraacetic acid; CCCP, carbonyl cyanide *m*-chlorophenylhydrazone; NPY, neuropeptide Y; GABA, γ-aminobutyric acid; fura-2/AM, fura-2 acetoxymethyl ester.

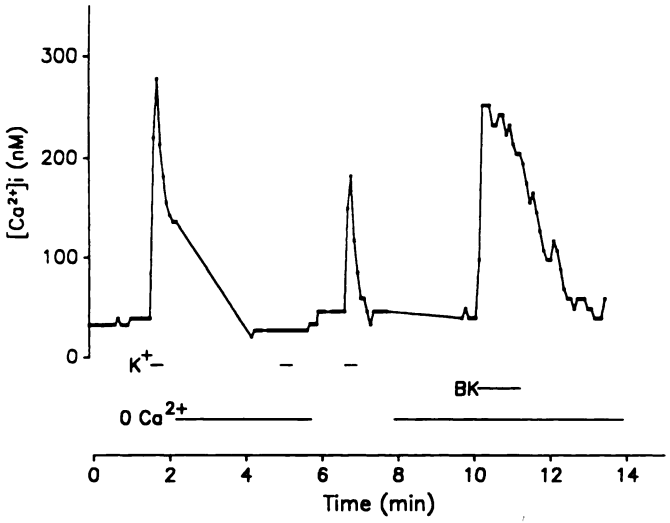

Fig. 1. Typical time course for the effects of 50 mM KCl solutions and BK (100 nM) on $[Ca^{2+}]_i$ in a fura-2/AM-loaded cell. These data were generated using the digital imaging paradigm illustrated in Fig. 2. Ca^{2+}-free solutions contained no added Ca^{2+} and 20 μM BAPTA. Solutions containing 50 mM KCl were substituted iso-osmotically for NaCl.

beam of light from a 200 W Hg arc lamp was passed through a dual-wavelength spectrophotometer (Phoenix Instruments, Philadelphia, PA), which alternated wavelengths from 340 to 380 nm by means of a spinning chopper (60 Hz). The light source was placed outside a darkened Faraday cage that enclosed a vibration isolation table supporting a microscope. A fused silica lens was positioned to focus light upon a liquid light guide (3 mm × 1 mm; Oriel, Stratford, CT) and a similar lens, placed at the terminating end of the guide, was positioned to direct light through the epifluorescent illuminator of the microscope. The light guide eliminated problems associated with vibration from the chopper and electrical noise from the arc lamp. The light was reflected off a dichroic mirror (Nikon DM 400) and focused through a 70× oil immersion objective (E. Leitz Inc., Rockleigh, NJ) (numerical apeture, 1.15). The emission fluorescence was selected for wavelengths with a 480-nm barrier filter and recordings were spatially defined with an adjustable rectangular diaphragm. The fluorescence emission was analyzed with a photomultiplier tube (bialkali) and discriminator (APED II; Thorn EMI Gencom Inc., Plainview, NY). The discriminator output was converted to pulses, which were then integrated by passing the signal through an eight-pole Bessel filter at 500 Hz. The gain on this detection system could be adjusted from 1- to 100-fold by increasing the pulse length. The conversion of light intensity to voltage by this process was confirmed to be linear over the range of the light levels used in these experiments. The signal from the filter was fed into one channel of an analog to digital convertor (PDP-11/73) computer system (Indec Systems, Sunnyvale, CA). The signals from two photodiodes, each placed in a small portion of the light beam directed toward the monochromators, were connected to two additional channels of the analog to digital convertor.

Sorting of the fluorescence output into signals corresponding to excitation at these two wavelengths was performed entirely by software written in BASIC-23 (Cheshire Data, Indec Systems). The photomultiplier output was sorted into signals from 340- and 380-nm excitation by using the photodiode outputs as timing signals and the output observed on-line throughout the experiment.

Cover slips (25-mm diameter), plated with cells, were mounted in the perfusion chamber (see Ref. 16), which was positioned on the opening of the microscope stage. The solution change in the cell superfusion system approximated a step occurring over 10 sec. The tubing between the large medium reservoirs and the inlet to the chambers delayed the onset of the solution change by an additional 10 sec. Figures have been corrected for the perfusion delay.

Calibration and analysis. Records were corrected for experimentally determined background values and the ratio of 340/380 nm fluorescence was calculated off-line. Ratios were converted to free Ca^{2+} by using the equation $Ca^{2+} = K(R - R_{min})(R_{max} - R)$, in which R is the 340/380 nm fluorescent ratio (14). The maximum ratio (R_{max}), the minimum ratio (R_{min}), and the constant K, the product of the dissociation product for fura-2 and the ratio of the free and bound forms of the dye at 380 nm, were determined from a fit to a standard curve, using the above equation, with a nonlinear least squares analysis computer program (15). The standard curve was determined for the fura-2 salt in calibration buffer (in mM: HEPES, 20; KCl, 120; NaCl, 5; $MgCl_2$, 1; pH 7.1) containing 10 mM EGTA, $K_s = 3.696 \times 10^6$ M^{-1} (18), with calculated amounts of Ca^{2+} added to give free calcium concentrations ranging between approximately 0 and 2000 nM. Identical calibration curves were obtained if CsCl was used to replace KCl. Experiments performed over long periods of time (>30 sec) were digitally filtered with an algorithm that added ½ the value of each data point to ¼ of the value of each neighboring point. The data were cycled through this routine five times. The $[Ca^{2+}]_i$ traces in patch-clamp experiments were digitally filtered by a single cycle through an 11-point moving average algorithm. For the digital imaging experiments, preloaded and washed cells (5 μM fura-2/AM for 30 min at 37°; washed for 40 min at the same temperature) were imaged according to methods previously described (16).

Cell culture. Neurons were cultured from the DRG of neonatal rats essentially as described previously (17). Briefly, DRG neurons were dissected from the thoracic and lumbar segments of 1–3-day-old Sprague-Dawley rats, incubated for 15 min at 37° in collagenase/dispase (0.8 and 0.4 units/ml), and then dissociated into single cells by trituration through a Pasteur pipette. The cells were then plated on laminin-fibronectin-coated coverglasses (25-mm diameter) and incubated in Ham's F-12 medium (GIBCO, Grand Island, NY), supplemented with 5% heat-inactivated rat serum, 4% 17-day embryonic extract, 50 ng/ml nerve growth factor, 44 mM glucose, 2 mM L-glutamine, 1% minimum essential medium, 100× vitamins, and penicillin/streptomycin (100 units/ml and 100 mg/ml, respectively), which was replaced every 2–3 days. Cultures were maintained at 37° in a water-saturated atmosphere with 5% CO_2. Cells between 3 and 10 days in culture were used for the present experiments.

Whole-cell patch clamp. The tight seal whole-cell configuration of the patch-clamp technique (18) was used to record transmembrane I_{Ca} from single cells while simultaneously measuring $[Ca^{2+}]_i$ transients. Cells were mounted in a perfusion chamber and thoroughly rinsed with a buffer composed of (in mM): tetraethylammonium chloride, 143; $CaCl_2$, 2; $MgCl_2$, 1; HEPES, 10; and glucose, 10; pH adjusted to 7.4 with tetraethylammonium hydroxide. A cell was then approached with a fire-polished pipette containing a solution composed of (in mM): fura-2 pentapotassium salt, 0.1; CsCl, 135; $MgCl_2$, 1; HEPES, 10; diTris phosphocreatinine, 14; MgATP, 3.6; and 50 units/ml creatinine phosphokinase; adjusted to pH 7.1 with CsOH. Current-clamp experiments were performed with a pipette solution composed of (in mM): fura-2 pentapotassium salt, 0.1; KCl, 135; $MgCl_2$, 1; HEPES, 10; diTris phosphocreatinine, 14; MgATP, 3.6; and 50 units/ml creatinine phosphokinase; adjusted to pH to 7.1 with KOH. The solutions perfusing cells in current-clamp conditions contained (in mM): NaCl, 138; $CaCl_2$, 2; $MgCl_2$, 1; KCl, 5; HEPES, 10; and glucose, 10; adjusted to pH 7.4 with NaOH. Action potentials were evoked by brief current pulses. Background fluorescence was recorded after formation of a gigaseal but before breaking into the cell, thus accounting for fluorescence contributed by the fura-2 in the pipette. Because the pipette approached the cell from above, the objective was focused below the pipette near the middle of the cell to minimize the pipette fluorescence. Fluorescent recordings were made from the cell soma alone. Full diffusion of the fura-2 into the cell occurs over a period of 1–3 min. Currents recorded by a Yale Mark V amplifier with a 1-GΩ feedback resistor were filtered by an eight-pole low-pass Bessel filter with a cutoff frequency of 200 Hz and were stored on a computer used for the fluorescence data

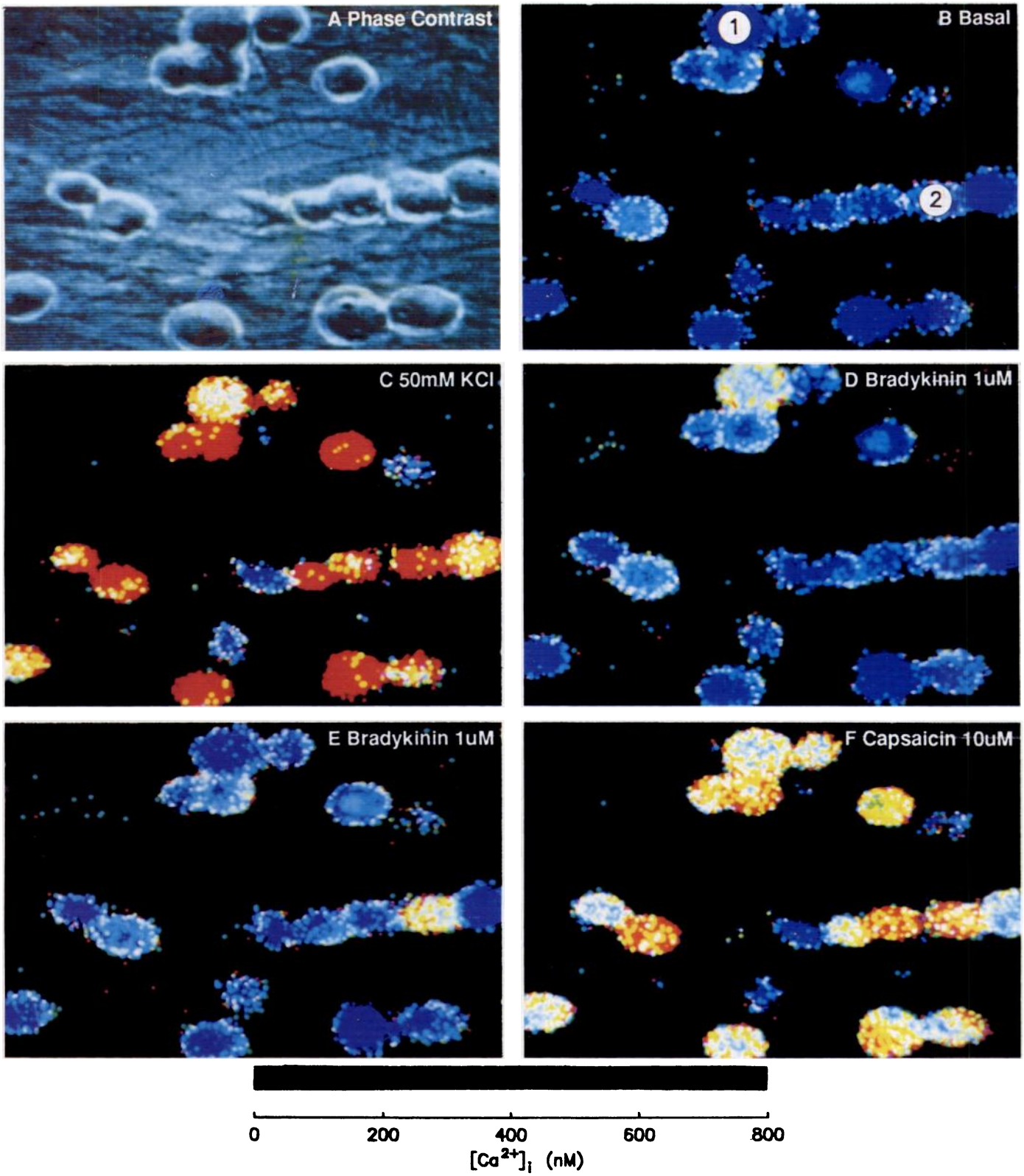

Fig. 2. Response of a representative field of cultured DRG cells to 50 mM KCl, 1 μM BK, and 10 μM capsaicin and the measurement of increases in $[Ca^{2+}]_i$ with fura-2/AM-based digital microfluorimetry. The time points representing the images B–F are also shown in Fig. 3. A, Phase contrast image of the DRG cells; B, basal $[Ca^{2+}]_i$ in these cells; C, ~85% of the cells challenged with 50 mM KCl solutions for 10 sec responded with an increase in $[Ca^{2+}]_i$; D and E, effect of perfusion with BK (1 μM) for 15 sec on $[Ca^{2+}]_i$; F, responses to capsaicin (10 μM) perfusion for 10 sec.

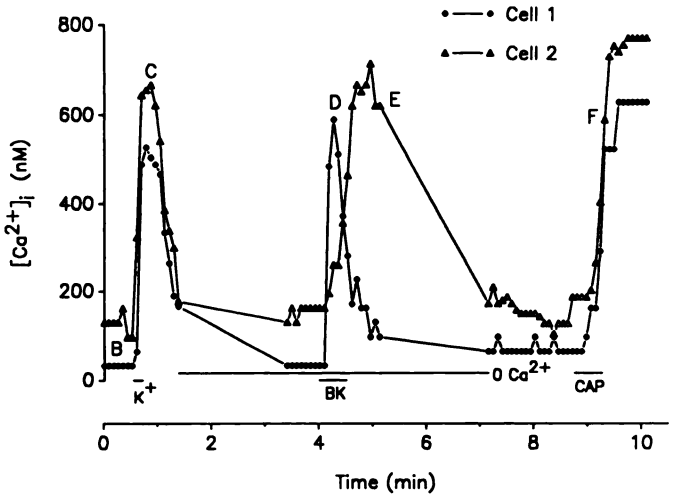

Fig. 3. Time course of two cells illustrated in Fig. 2 that responded to 1 μM BK as shown in Fig. 2, and to the application of 50 mM KCl and 10 μM capsaicin (*CAP*). ●, Cell labeled *1* in Fig. 2B; △, time course of cell labeled *2* in the same figure.

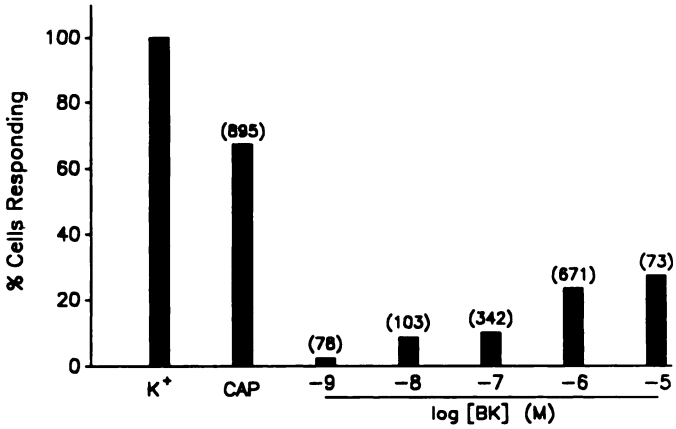

Fig. 4. Number of cells responding to capsaicin (10 μM) (*CAP*) and various concentrations of BK in Ca^{2+}-free solutions with an increase in $[Ca^{2+}]_i$. *Numbers in parenthesis above each column*, number of cells in which the increases in $[Ca^{2+}]_i$ were observed. The values have been normalized to 50 mM KCl-sensitive cells (approximately 95% of cells present). The criterion for responding cells was an observed 50% increase in basal $[Ca^{2+}]_i$.

acquisition. Linear leak corrections were performed by averaging 16 10-mV hyperpolarizing pulses from the holding potential. The DC component of the averaged leak current was then modelled so as to increase the signal to noise ratio. Digital summation of this leak template after appropriate scaling with the current obtained during depolarizing test pulses provided the leak correction. Series resistance compensation of approximately 40% was possible with the uncompensated portion of the series resistance ranged between 1.8 and 3 MΩ Peak I_{Ca} and I_{Ba} values rarely exceeded 1.5 or 2.5 nA, respectively, giving approximate maximum voltage errors of 4.5 and 7.5 mV. Cells were discarded when the steady leakage current at the holding potential was greater than 5% of the peak inward current. All experiments were performed at room temperature.

Data analysis. In the presence of potassium channel-blocking medium and in the absence of $[Ca^{2+}]_i$ chelators in the patch pipette, I_{Ca}'s are observed to decline, particularly for high stimulus intensities that produce larger loads of $[Ca^{2+}]_i$ (see Fig. 6C). In order to account for the rate of rundown as a factor in calculating the inhibition of the $[Ca^{2+}]_i$ and the current parameters, the peak I_{Ca}, the integral of the I_{Ca}, and the net $[Ca^{2+}]_i$ rise were plotted as a function of time for at least three sweeps before addition of BK. This time course was then plotted as a linear function and the decline was extrapolated to the point at which maximum effects of BK were observed. The expected magnitudes of the parameters shown were then used to calculate the inhibition produced.

Materials. All reagents were of Analar grade. Fura-2 pentapotassium salt was obtained from Molecular Probes Inc. (Eugene, OR). BK and other agents were obtained from Sigma Chemical Co.

Results

BK-induced Ca^{2+} mobilization. BK has been shown to stimulate inositol trisphosphate production in cultures of rat DRG neurons (19). This results in Ca^{2+} mobilization from intracellular stores. Fig. 1 shows a typical time course for the response of a single DRG cell to a 50 mM KCl-evoked depolarization in the presence of 2 mM extracellular Ca^{2+}, as determined by digital imaging of fura-2/AM-loaded cells. The majority of cells examined by this method were found to respond to 50 mM KCl-induced depolarization with an increase in $[Ca^{2+}]_i$ (see also Figs. 2, 3, and 4 for summary). As would be anticipated, in the absence of extracellular Ca^{2+} (with 20 μM BAPTA added), 50 mM KCl failed to increase $[Ca^{2+}]_i$ (Fig. 1). In order to unambiguously estimate the number of cells that responded to BK by increasing $[Ca^{2+}]_i$ through mobilization from intracellular stores, cells were perfused with BK in Ca^{2+}-free solutions. From the typical time course illustrated in Fig. 1, it may be seen that in some cells BK clearly produced an increase in $[Ca^{2+}]_i$ in the absence of extracellular Ca^{2+}. Recovery of the increase in $[Ca^{2+}]_i$ was complete for all cells that responded. Further effects of BK on $[Ca^{2+}]_i$ may also be seen in the color images presented in Fig. 2. The response to 50 mM KCl was observed in >95% of DRG cells (Figs. 1–4). However, in Ca^{2+}-free solutions BK (1 μM) increased $[Ca^{2+}]_i$ in markedly fewer cells. Fig. 2 also illustrates that a number of cells in these cultures responded to superfusion with 10 μM capsaicin by an increase in $[Ca^{2+}]_i$. Capsaicin has been shown to selectively stimulate sensory nociceptive neurons through the formation of a channel that is highly permeable to both Na^+ and Ca^{2+} (20). Fig. 3 shows the time course of the responses to 50 mM KCl, BK (1 μM), and capsaicin (10 μM) in two cells identified in Fig. 2. Fig. 4 summarizes data collected from several DRG cell cultures and provides a dose-response curve for BK-induced Ca^{2+} mobilization. The data are expressed as percentage of cells responding to KCl-dependent depolarization. The results demonstrate that capsaicin (10 μM) produced an increase in $[Ca^{2+}]_i$ in approximately 65% of the DRG cells in culture. Of those cells that responded to BK (100 nM) (approximately 10–15% of the total cells present), 85% were also capsaicin sensitive (86% for 1 μM BK).

BK effects on Ca^{2+} currents. BK has been previously shown to inhibit the I_{Ca} in DRG cells, using EGTA as an intracellular Ca^{2+} chelator and Ca^{2+} as the charge carrier (5). Fig. 5A, *upper* illustrates an example of the inhibition of the I_{Ca} by BK (100 nM), using extracellular Ba^{2+} as the charge carrier and buffering of $[Ca^{2+}]_i$ with 20 mM BAPTA. The first application of BK (100 nM for 30 sec) produced a 20% inhibition of the I_{Ba}. The degree of recovery from the effects of BK in this particular cell was almost complete, although if the duration of perfusion was increased to 2 min the degree of recovery was slower and reduced. The mean BK-dependent inhibition of the I_{Ba} for a 2-min application was 24 ± 6% for the 7 of the 11 cells tested that responded. The mean recovery for these 7 cells was

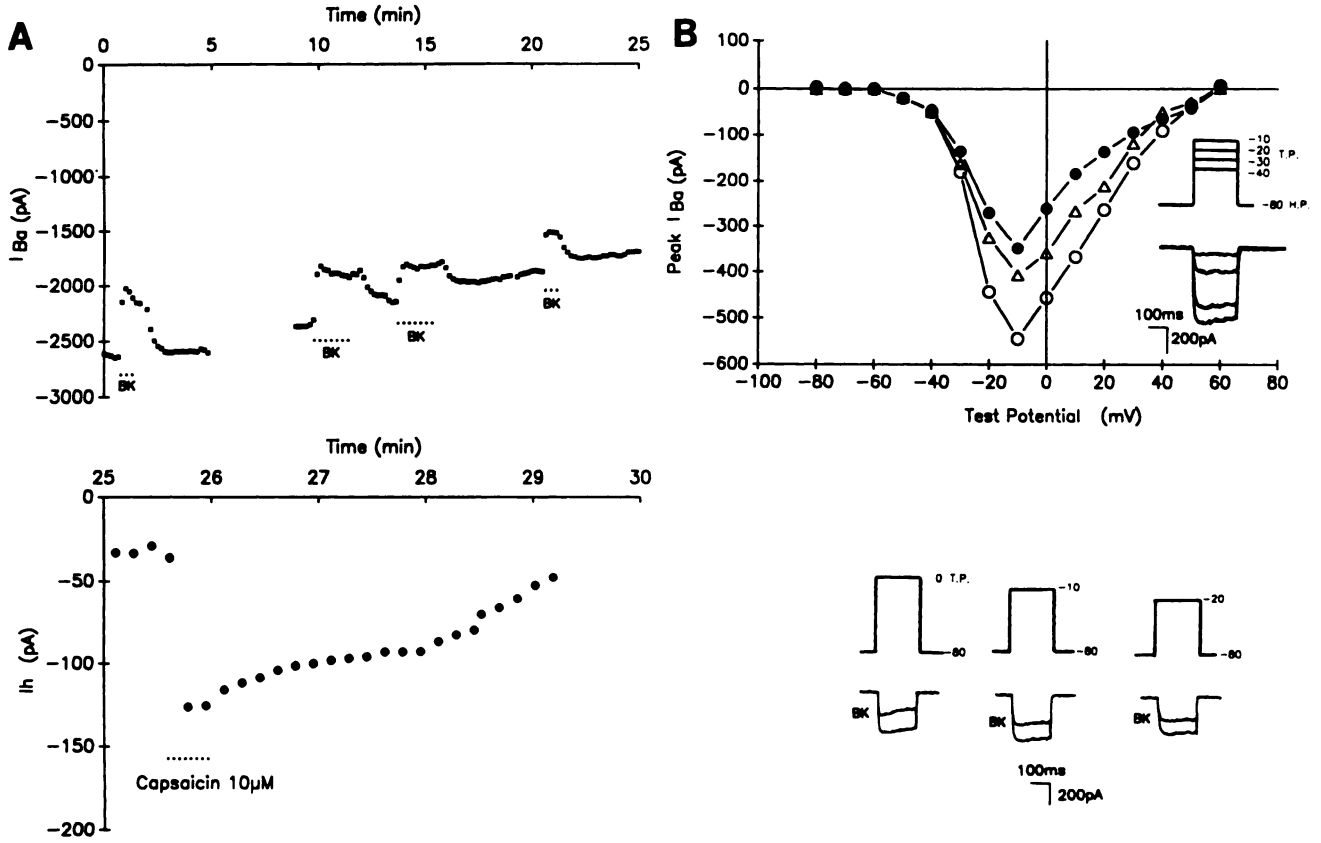

Fig. 5. A, *Upper*, time course of the effect of BK on the I_{Ba}, using 2 mM Ba^{2+} as the charge carrier, in the presence of 20 mM BAPTA in the patch pipette. BK (100 nM) was applied by superfusion for either 30 sec or 2 min. *Lower*, the effect of capsaicin (10 μM) was examined on the DRG cell shown in *upper* and the capsaicin-dependent increase in the holding current (*Ih*) that occurs is shown. B, *Upper*, current-voltage relationship for the effect of BK (100 nM) on the I_{Ba}, measured in the presence of 20 mM BAPTA in the patch pipette. The *traces* show the current-voltage relationship from a holding potential of −80 mV in the absence (○) and presence (●) of BK (100 nM) and following washout of the peptide for 2 min (△). *Lower*, individual current records, in the absence and presence of BK (100 nM), plotted in *upper*. *T.P.*, test potential; *H.P.*, holding potential.

55 ± 6%. Fig. 5A, *lower* shows that this cell also responded to capsaicin, as indicated by an increase in the holding current that results from an increase in the membrane conductance previously described (21). Fig. 5B shows the current-voltage relationship for the effect of BK on the I_{Ba}, demonstrating that there appeared to be no apparent change in the voltage dependence for activation of the I_{Ca} over the voltage range examined. Because BK inhibited the I_{Ca} (5) or I_{Ba} in many more DRG neurons than in which it mobilized Ca^{2+} from intracellular stores (Fig. 4 and see below) and even produced these effects when $[Ca^{2+}]_i$ was buffered with EGTA (5) or 20 mM BAPTA (see above), it is clear that in the majority of cases BK inhibition of the I_{Ca} is not the result of BK-induced Ca^{2+} mobilization but represents a separate process.

Combined voltage-clamp/$[Ca^{2+}]_i$ measurements. We further investigated the relationship between the effect of BK on the I_{Ca} and $[Ca^{2+}]_i$ by simultaneously monitoring the I_{Ca} and $[Ca^{2+}]_i$ in single DRG cells under voltage-clamp conditions. Depolarizing voltage clamp steps of varying durations (10–640 msec) from a holding potential of −80 mV to a test potential of 0 mV were applied to DRG neurons, as shown in Fig. 6A. Fig. 6A, *upper trace* illustrates the resulting rise in $[Ca^{2+}]_i$ and the *lower trace*, the associated I_{Ca}. In the cell illustrated, the $[Ca^{2+}]_i$ increased from a basal level of 100 nM to a peak of 700 nM during the 640-msec depolarizing pulse. The mean basal $[Ca^{2+}]_i$ for the DRG neurons examined in this series of experiments was 131 ± 7 nM (n = 102 cells). Several features of the $[Ca^{2+}]_i$ transients were apparent. (a) Longer test pulse durations resulted in $[Ca^{2+}]_i$ transients of increasing amplitude. However, for the longest test pulse durations the increase in $[Ca^{2+}]_i$ produced was no longer proportional to the integral of the I_{Ca}. (b) The rise in $[Ca^{2+}]_i$ was buffered slowly following depolarization but not during the depolarizing step. The return to basal $[Ca^{2+}]_i$ took approximately 20–30 sec.

The effect of voltage steps of increased duration is illustrated in Fig. 6B, where the test pulse duration and the concomitant rise in the $[Ca^{2+}]_i$ are plotted. The figure shows that the rise in $[Ca^{2+}]_i$ reached an asymptote at long test pulse durations. Because inactivation of the I_{Ca} occurs in these cells during the depolarizing step, the integral of the I_{Ca} was also plotted against the net $[Ca^{2+}]_i$ (Fig. 6C). The resulting curve is comparable to that shown for the increase in $[Ca^{2+}]_i$ for given test pulse durations (Fig. 6B). For values of test pulse durations up to 160 msec, the relationship between either the integral of the I_{Ca} or the test pulse duration and $[Ca^{2+}]_i$ was essentially linear. Hence, it appears that, when a larger Ca^{2+} load is imposed on the DRG cell, it is more effectively buffered than a smaller load. This is consistent with the increased buffering capacity at higher $[Ca^{2+}]_i$ that we have previously observed in DRG cells (22) and that has also been observed in molluscan neurons (23) and in smooth muscle cells (24). Experiments were also performed in order to establish whether the peak $[Ca^{2+}]_i$ values attained on formation of the asymptote could be readily exceeded. Fig. 6D, *upper* illustrates a cell in which the asymptote was reached at

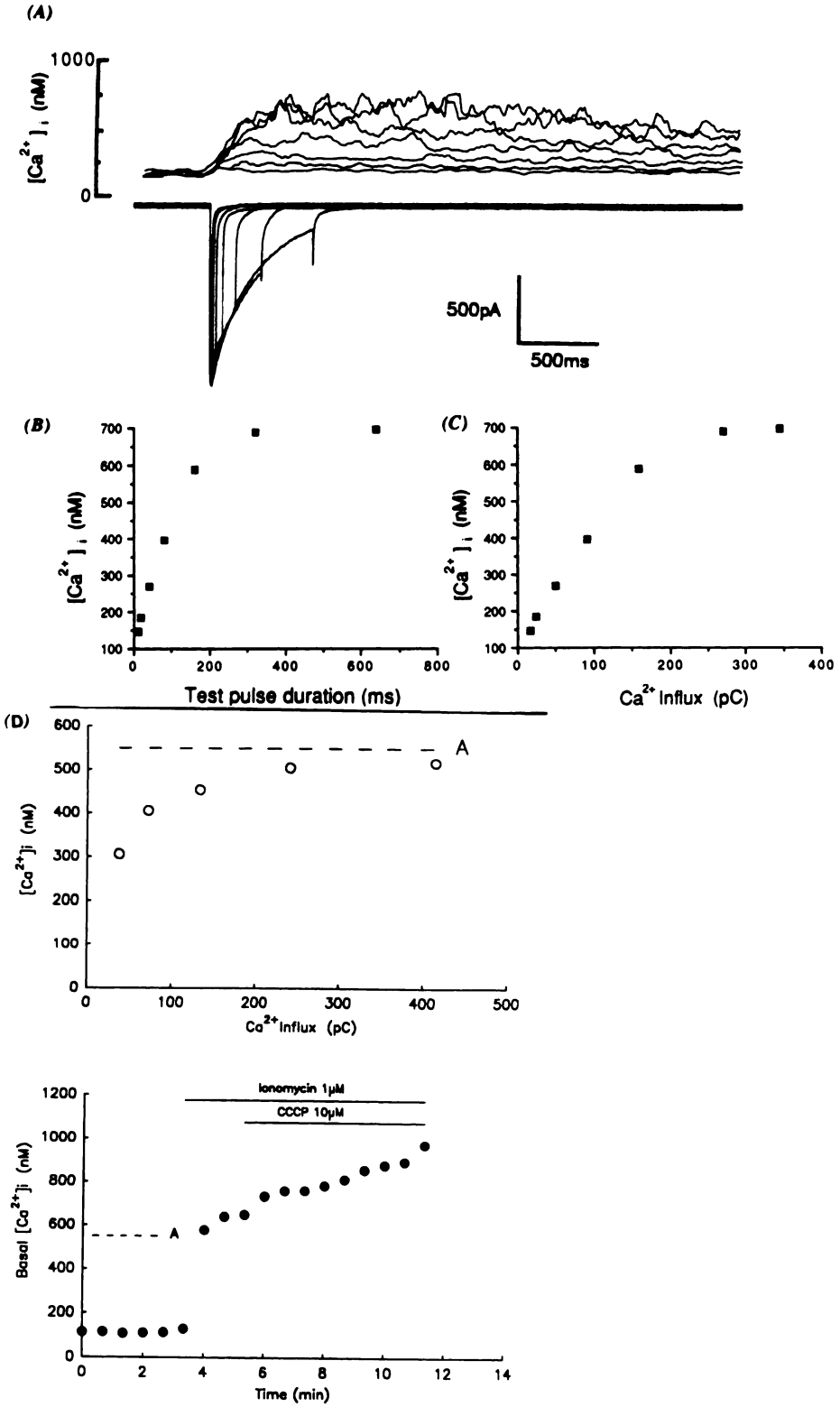

Fig. 6. A, Increase in the amplitude of the $[Ca^{2+}]_i$ transient in a rat DRG cell in response to step depolarizations from a holding potential of −80 mV to a test potential of 0 mV for durations that vary between 10 and 640 msec, using the whole-cell voltage clamp technique and simultaneous measurement of fura-2 (100 μM) fluorescent intensities of 340- and 380-nm excitation and 510-nm emission. B, Relationship between the net $[Ca^{2+}]_i$ (peak minus basal $[Ca^{2+}]_i$) and test pulse duration obtained from A. C, Relationship between the net $[Ca^{2+}]_i$ and the total Ca^{2+} influx (*pC*, integral of the inward current during the test pulse) obtained from A. Recordings were made at 40-sec intervals. D, *Upper*, relationship between Ca^{2+} influx and $[Ca^{2+}]$ (peak value) in a single DRG cell, produced by depolarization of the cell from −80 mV to 0 mV for various durations (range, 40 to 1280 msec). An asymptote, as illustrated in B, was reached on increasing Ca^{2+} influx. *A*, $[Ca^{2+}]$ value slightly above this asymptote. The cell shown was then perfused with solutions containing ionomycin (1 μM) and CCCP (10 μM) as denoted by the *horizontal bars* and shown in *lower*. *Lower*, time course of the basal $[Ca^{2+}]_i$ during (– – –) and following formation of the asymptote shown in *upper*. The level at which the asymptote was reached is denoted by *A*, as in *upper*. Following perfusion with ionomycin (1 μM) and CCCP (10 μM), the $[Ca^{2+}]_i$ increased to > 1 μM within 8 min.

a $[Ca^{2+}]_i$ value of 500 nM. Following the formation of this asymptote, the same cell was superfused with solutions containing the calcium ionophore ionomycin (1 μM) and the mitochondrial uncoupling agent CCCP (10 μM) (Fig. 6D, *lower*). CCCP has previously been shown to disrupt mitochondrial sequestration of $[Ca^{2+}]_i$ in DRG cells (22). Under these conditions the $[Ca^{2+}]_i$ exceeded a value of 1 μM within 8 min of superfusion with these agents. This demonstrates that the formation of the asymptote was not due to saturation of the fura-2 signal.

The BK-induced rise in basal $[Ca^{2+}]_i$ observed in the fura-2/AM imaging experiments was also observed in cells using combined patch-clamp/fura-2-based microfluorimetry. Sixteen cells responded in this way of 102 tested (data not shown). The mean BK-dependent increase in $[Ca^{2+}]_i$ in the responding cells was from 146 ± 37 to 271 ± 52 nM (for these voltage-clamp

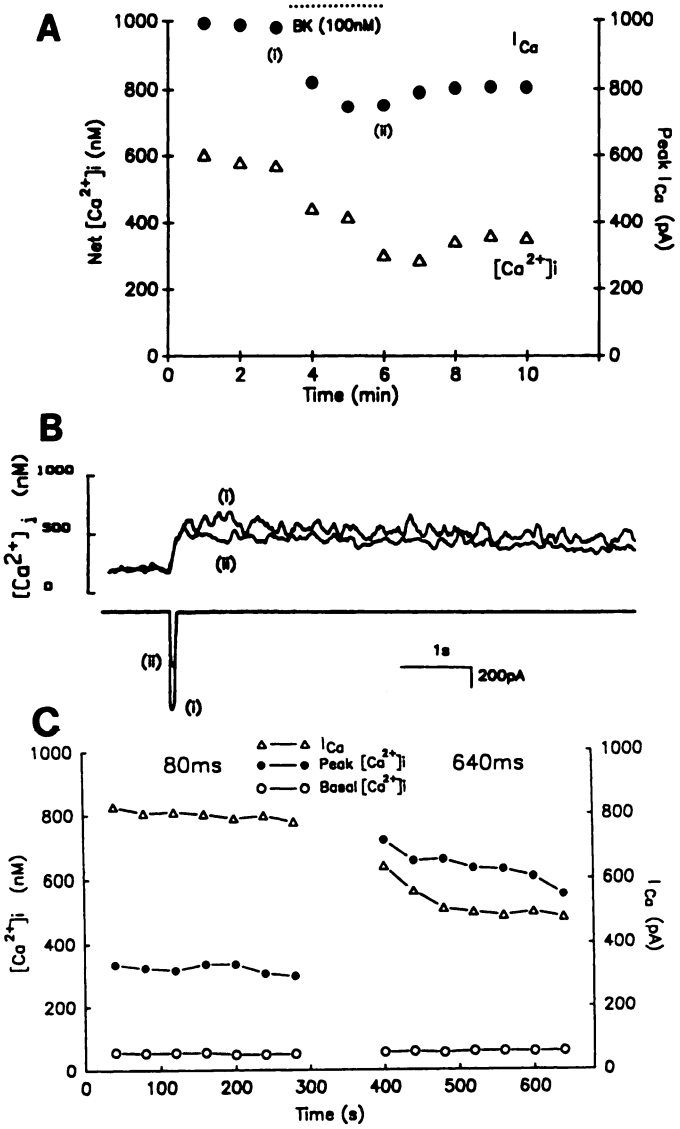

Fig. 7. A, Effect of BK (100 nM) on the magnitude of the net $[Ca^{2+}]_i$ transient (△) in a rat DRG cell in response to step depolarizations from a holding potential of −80 mV to a test potential of 0 mV, for a duration of 80 msec, and on the I_{Ca} (●), as measured simultaneously using combined patch-clamp microfluorimetry. B, Individual records of $[Ca^{2+}]_i$ transients and I_{Ca} from A at time points (*i* and (*ii*). C, Time-dependent decline in the amplitude of the peak $[Ca^{2+}]_i$ transient (●) and I_{Ca} (△) that results from step depolarizations from a holding potential of −80 mV to a test potential of 0 mV for 80- or 640-msec duration. The basal $[Ca^{2+}]_i$ is also shown (○). To account for the rate of rundown as a factor in calculating the inhibition of the $[Ca^{2+}]_i$ and the current parameters, the peak I_{Ca} and the net $[Ca^{2+}]_i$ rise were plotted as a function of time for at least three sweeps before the addition of BK (100 nM). This time course was then plotted as a linear function and the decline was extrapolated to the point at which maximum effects of BK were observed to occur within 3 min of perfusion. The expected magnitudes of the parameters shown were then used to calculate the inhibition produced.

studies the cell was considered as responding if the $[Ca^{2+}]_i$ increased by at least 50%). BK also reduced the I_{Ca} in 54 of 79 cells examined under simultaneous patch-clamp/fura-2-based microfluorimetric conditions. Thus, in most neurons BK reduced the I_{Ca} without producing an increase in the basal $[Ca^{2+}]_i$. Together with the other data presented above, we believe that this suggests that the two effects are not necessarily causally related.

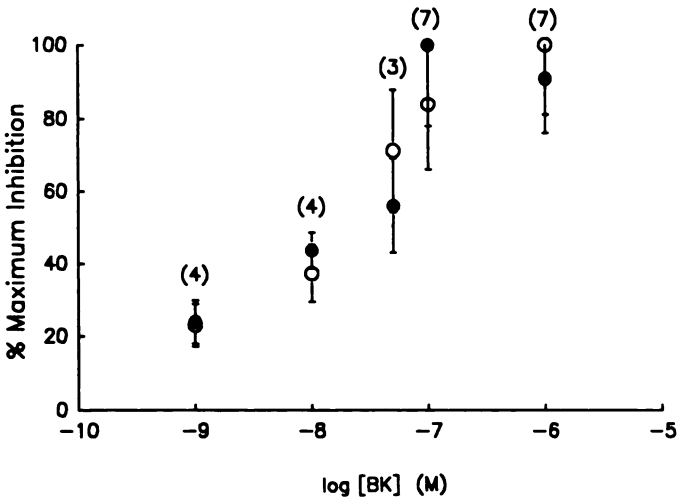

Fig. 8. Dose-response curves for the BK-induced inhibition of the I_{Ca} (○) and the accompanying rise in $[Ca^{2+}]_i$ (●) in single rat DRG cells (see legend to Fig. 7C and Materials and Methods for method of analysis). *Numbers in parenthesis*, number of cells in which an effect of BK at a particular concentration was observed; *vertical bars*, standard error for these observations.

The mean inhibition of the I_{Ca} by BK (100 nM) was 31 ± 4% (n = 38 cells). Fig. 7, A and B, illustrates a cell in which the I_{Ca} and the $[Ca^{2+}]_i$ resulting from the depolarizing step from −80 mV to 0 mV were both reduced. Recovery of the BK effects on the I_{Ca} was >75% in only 40% of cells examined under these recording conditions (25–50% recovery in 40% of cells and less than 25% recovery in 20% of cells was observed). Repeated application of BK also resulted in a considerably reduced response, indicating a certain degree of desensitization (data not shown).

In order to quantify the effects of BK on both the I_{Ca} and $[Ca^{2+}]_i$ in single DRG cells under voltage-clamp conditions, it was necessary to account for the time-dependent rundown of the I_{Ca} and $[Ca^{2+}]_i$ by linear extrapolation from prestimulated control values. Such rundown is a common problem associated with recording in the presence of K^+ channel-blocking agents and when the $[Ca^{2+}]_i$ is unbuffered, as is illustrated in Fig. 7C (for details of data analysis, see Materials and Methods).

In a number of cells the effects of both BK and capsaicin were examined. We have shown elsewhere that capsaicin produces a change in holding current, inhibition of the I_{Ca} and an increase in $[Ca^{2+}]_i$ (21) (Fig. 5A, *lower*). Of six cells tested with both agents under voltage-clamp conditions, capsaicin (10 μM) produced a change in the aforementioned parameters in five cells. In four of the five cells that responded to capsaicin, BK produced a decrease in the I_{Ca} in the absence of a detectable change in $[Ca^{2+}]_i$. These results indicate that the inhibitory effect of BK on the I_{Ca} frequently occurs in capsaicin-sensitive DRG cells, which are thought to represent nociceptive neurons.

The effects of BK on both the I_{Ca} and the accompanying $[Ca^{2+}]_i$ were concentration dependent. Fig. 8 shows the relationship between the concentration of BK and the inhibition of these parameters, yielding an IC_{50} value of approximately 20 nM in both cases. This appears to be somewhat lower than that for BK-induced Ca^{2+} mobilization (Fig. 4).

We investigated the relationship between the inhibitory effect of BK on the I_{Ca} and its effects on $[Ca^{2+}]_i$ transients produced by depolarizing voltage steps of different durations.

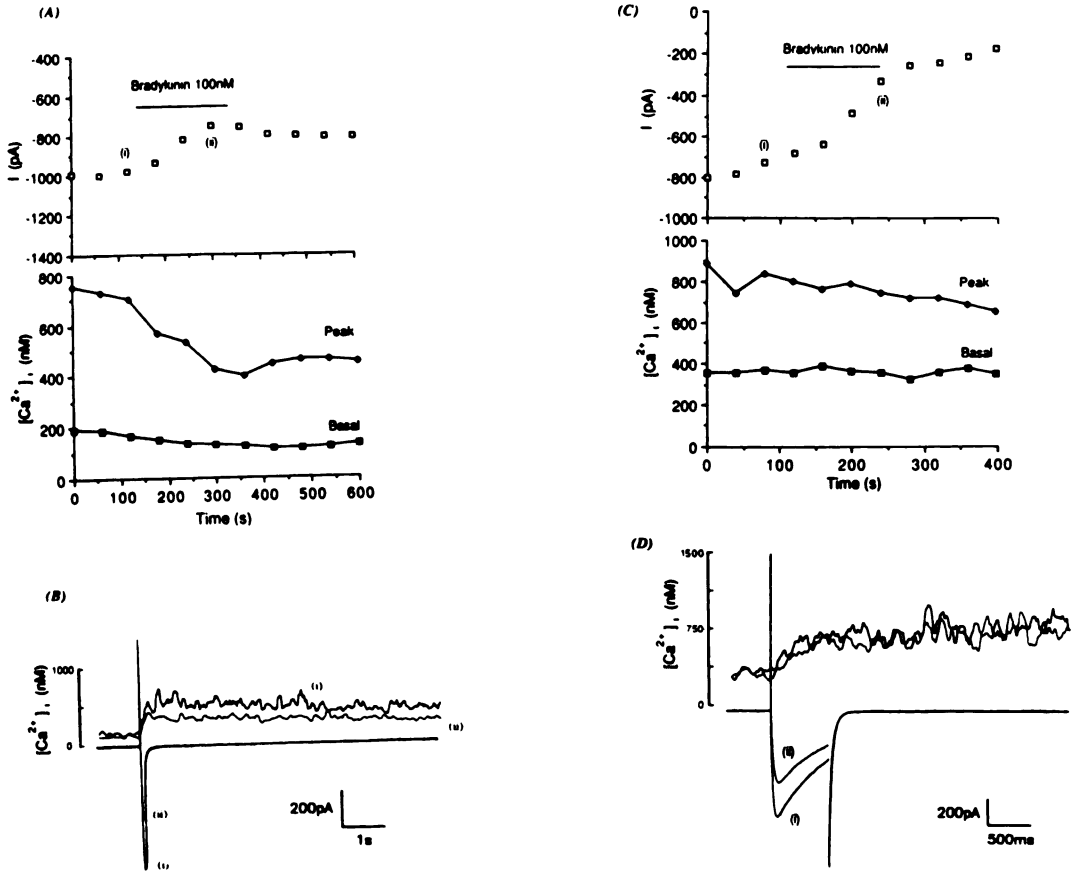

Fig. 9. A, Basal (■) and peak $[Ca^{2+}]_i$ (●) associated with 160-msec depolarizations from −80 to 0 mV every 60 sec. *Upper*, magnitude of the peak I_{Ca} (□); *horizontal bar*, presence of BK (100 nM); (*i*) and (*ii*), traces shown in B. B, *Lower traces*, I_{Ca}; *upper traces*, $[Ca^{2+}]_i$ transients for the time points indicated in A. (*i*) and (*ii*), depolarizations in the absence and presence of 100 nM BK, respectively. C, Basal (■) and peak $[Ca^{2+}]_i$ (●) associated with 640-msec depolarizations from −80 to 0 mV every 40 sec, in a different cell than that shown in A. *Upper trace*, peak I_{Ca} (□) for each depolarization; *horizontal bar*, presence of BK (100 nM); (*i*) and (*ii*), time points shown in detail in B. D, *Lower traces*, I_{Ca}, in the absence [(*i*)] and in the presence of BK (100 nM) [(*ii*)]. *Upper traces*, associated rise in $[Ca^{2+}]_i$ for the sweeps shown.

Fig. 9A illustrates a DRG cell that was depolarized from a −80-mV holding potential to 0-mV test potential for 160 msec at 40-sec intervals, in which the I_{Ca} and rise in $[Ca^{2+}]_i$ were recorded. On application of a solution containing BK (100 nM), both the I_{Ca} and the amplitude of the corresponding increase in $[Ca^{2+}]_i$ were reduced. The individual records for the time points marked in Fig. 9A are shown in Fig. 9B, illustrating a marked inhibition of both the I_{Ca} and the amplitude of the $[Ca^{2+}]_i$ transient. Results for a different cell, where the test pulse duration was 640 msec, are shown in Fig. 9, C and D. In Fig. 9C it can be seen that BK produced a marked inhibition of the I_{Ca} in this cell as well. However, there was no significant inhibition of the amplitude of the corresponding rise in $[Ca^{2+}]_i$. Fig. 9D shows individual records of the time points indicated in Fig. 9C. Combined results from several similar experiments are plotted in Fig. 10. Although the test pulse durations at which the asymptotic portion of any curve was reached and the magnitude of the inhibitory response to BK varied somewhat from cell to cell, it is clear from Fig. 10, *upper*, that there was a differential effect of BK on the net increase in $[Ca^{2+}]_i$, which was dependent upon the duration of depolarization and, consequently, the level of $[Ca^{2+}]_i$ reached. Fig. 10, *middle* and *lower* show the inhibition of the peak I_{Ca} and the integral of the I_{Ca}, respectively, for the data plotted in Fig. 10, *upper*, demonstrating that BK inhibited both parameters by a similar amount for any given test pulse duration.

Effect of BK on $[Ca^{2+}]_i$ during current-clamp recordings. The $[Ca^{2+}]_i$ asymptote observed during the voltage-clamp experiments was also observed when action potentials were elicited in DRG cells by brief current injections for cells in whole-cell current clamp. The resting membrane potential of the DRG cells examined ranged between −50 and −60 mV. In these experiments, the membrane potential was adjusted to approximately −60 mV by current injection. Firing of one action potential produced a small but long lasting increase in $[Ca^{2+}]_i$. Several action potentials fired in succession produced a stepwise increase in $[Ca^{2+}]_i$ (Fig. 11A). In an analogous fashion to the effect of increasing the duration of depolarizing steps under voltage clamp, we found that, when the number of action potentials in a given train was increased, the resulting increase in $[Ca^{2+}]_i$ reached an asymptote (Fig. 11B). This effect was variable from cell to cell, with the asymptote being obtained for between 15 and 50 action potentials in a train. BK (100 nM) transiently depolarized ~62% (n = 15) of the cells examined from a mean adjusted membrane potential of −60.7 ± 1.3 mV to −52.8 ± 2.2 mV (n = 15 of the 24 cells examined). This BK-induced depolarization was rapidly reversed upon washout of the peptide. BK also inhibited the rise in $[Ca^{2+}]_i$ resulting from the repetitive firing of action potentials. The effect of BK (100 nM) on the $[Ca^{2+}]_i$ response produced by a train of action potentials can be seen in Fig. 12. A train of action potentials was evoked every 40 sec and the rise in $[Ca^{2+}]_i$ was recorded. After perfusion of the cell for 2 min with BK (100 nM), there was a significant reduction in the peak rise in $[Ca^{2+}]_i$. This effect of BK was also observed in ~60% of the cells examined under current-clamp conditions (15 of 24 cells). Fig. 13 illustrates an experiment in which the effects of BK (100 nM) on the rise in $[Ca^{2}]_i$ produced in a DRG cell by short and long

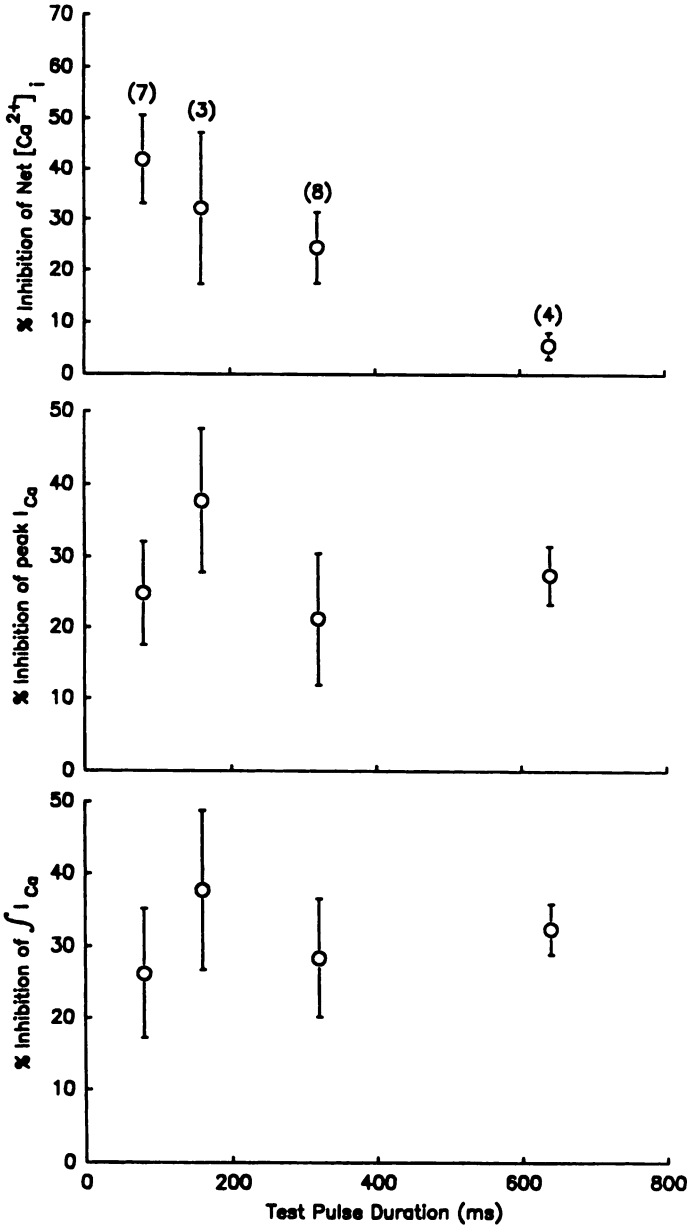

Fig. 10. Data from several DRG cells showing the percentage of inhibition of the maximum net increase in $[Ca^{2+}]_i$ (*upper*), inhibition of the peak I_{Ca} (*middle*), and inhibition of the integral of the I_{Ca} (*lower*) for different test pulse durations by 100 nM BK. (To account for the rate of rundown as a factor in calculating the inhibition of the $[Ca^{2+}]_i$ and the current parameters, see legend to Fig. 7C). *Numbers in parenthesis*, the number of observations for each pulse duration; *vertical bars*, standard error of these observations.

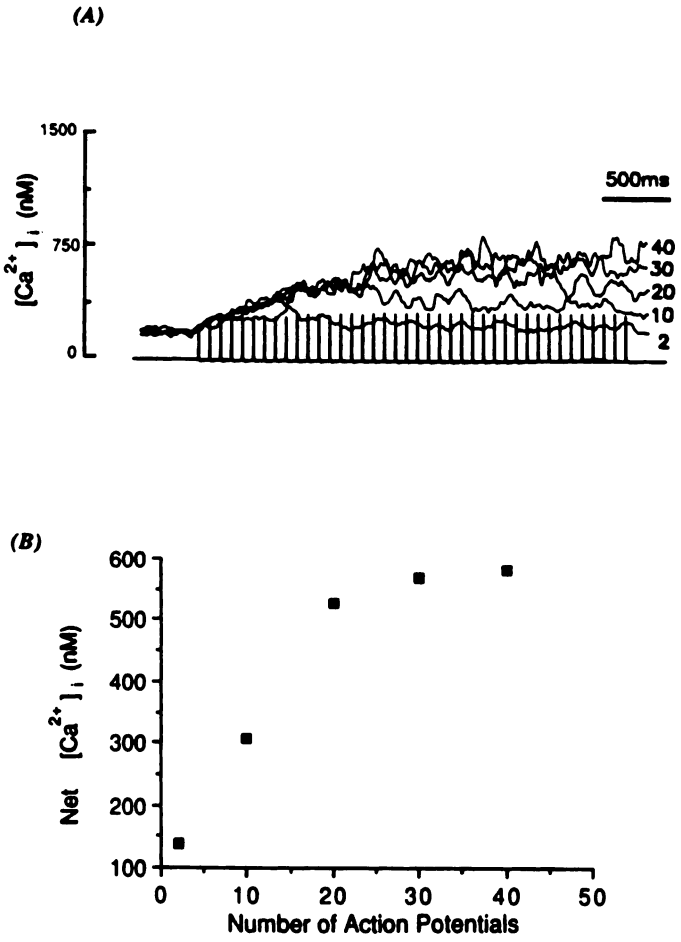

Fig. 11. A, Simultaneous current-clamp and $[Ca^{2+}]_i$ recordings from a DRG cell. The rise in $[Ca^{2+}]_i$ was due to action potentials elicited by repeated injections of 890 pA of current for 4 msec. *Traces 1–5*, 2, 10, 20, 30, and 40 action potentials in a train (12.5 Hz), respectively, with 40 sec between each series of current injections from the same cell. B, Asymptote in $[Ca^{2+}]_i$ reached resulting from action potentials evoked by the current injection shown in A.

trains of action potentials were examined. It can be seen that the inhibition of the $[Ca^{2+}]_i$ transient associated with the shorter train (10 action potentials) (Fig. 13B) was larger than for the longer train (40 action potentials) (Fig. 13). For between 5 and 15 action potentials fired, the mean maximal inhibition of the amplitude of the $[Ca^{2+}]_i$ transient produced by BK was 42.4 ± 4.7% (10 observations from seven cells). For between 30 and 35 action potentials fired in the same set of cells in which these BK effects were observed, the mean inhibition of the $[Ca^{2+}]_i$ signal was 17.2 ± 5.6% (seven observations from seven cells). In all of these cells at least partial recovery from the effects of BK was observed, as illustrated in Fig. 12. However, as with inhibition of the I_{Ca} (see above and Fig. 6A), the extent of this recovery was somewhat variable from cell to cell, at least during the time course of the experiment.

Because the BK-induced depolarization was fairly slow in onset, it was possible to maintain the membrane potential at its initial value by adjustment of the injected current between successive sweeps. Following this protocol, BK still differentially modulated $[Ca^{2+}]_i$ signals in response to short action potential trains when the membrane potential was maintained at approximately −60 mV.

Discussion

Although it is well established that BK excites some populations of sensory neurons, the mechanism by which this occurs is unclear (2, 3). We have demonstrated that BK reduces the depolarization-activated influx of Ca^{2+} into DRG cells. These effects of BK seem to frequently occur in capsaicin-sensitive cells, which are probably sensory nociceptors. In addition, BK mobilizes Ca^{2+} from intracellular stores in a subpopulation of neurons. We propose that BK inhibition of depolarization-induced Ca^{2+} influx may make a contribution to BK-induced excitation of these cells.

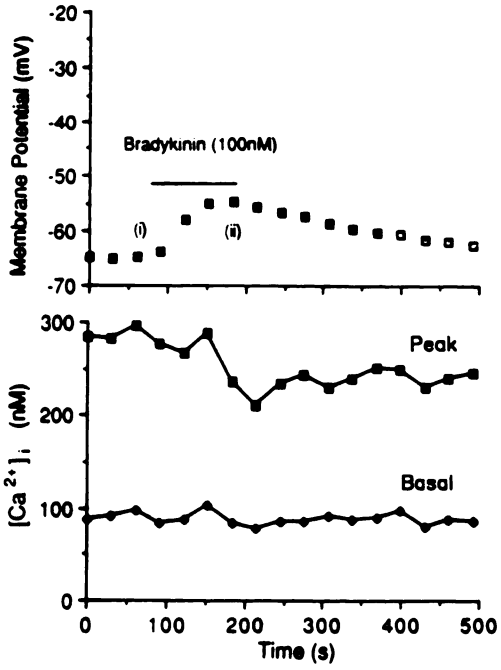

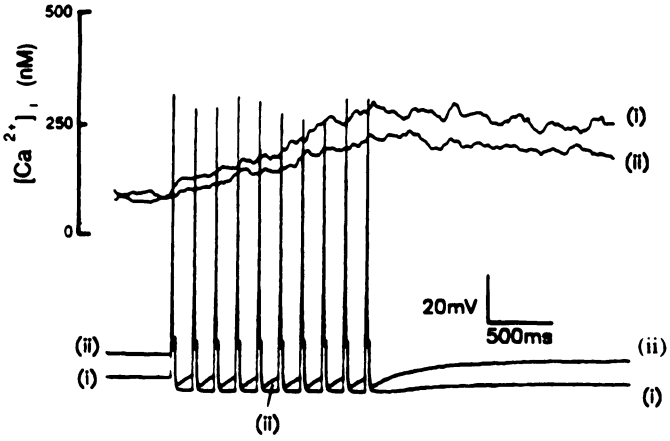

Fig. 12. A, Current-clamp studies of DRG cells showing the BK (100 nM)-dependent depolarization and inhibition of the rise in $[Ca^{2+}]_i$ associated with the firing of 10 action potentials (6.25 Hz) (■, peak; ●, basal). In this example the cell membrane potential was readjusted to −65 mV before measurement of the first time point. *Upper*, BK-dependent depolarization (⊡). B, *Lower*, action potentials for the sweeps indicated in the *main panel* and the $[Ca^{2+}]_i$ transient for these sweeps. In this particular cell there was a slow afterhyperpolarization (observed in 35% of cells), which was reduced upon addition of BK. Current injection was 550 pA for 32 msec to elicit the action potentials. *Vertical scale*, 20 mV; *Horizontal scale*, 500 msec. (*i*), 10 action potentials fired in the absence, and (*ii*), in the presence, of 100 nM BK. *Horizontal bar*, perfusion with BK (100 nM). The firing frequency was 12.5 Hz.

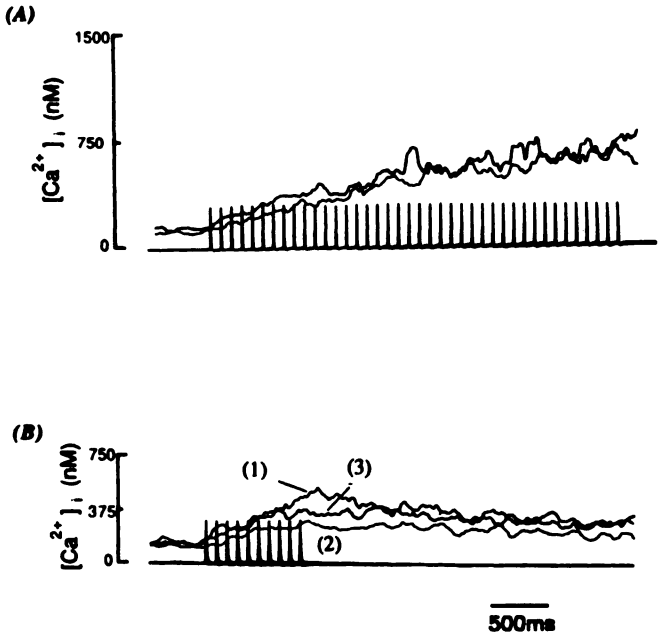

Fig. 13. A, Effect of BK (100 nM) on 40 action potentials fired, showing no significant reduction in peak $[Ca^{2+}]_i$ produced by BK. The firing frequency was 12.5 Hz. Note the converging $[Ca^{2+}]_i$ signals for increasing numbers of action potentials in the train. B, In the same cell as A, individual sweeps of 10 action potentials fired in the absence [(*1*)] or presence [(*2*)] of 100 nM BK, and the recovery [(*3*)] following removal of the peptide. In the cell shown the current injected was 700 pA for 8 msec.

Several actions of BK have been previously identified that have also been proposed to contribute to its excitatory actions. These include the depolarizing effect of the peptide (7), which we have also observed in the present series of experiments. Rang and Ritchie (8) have demonstrated that BK-induced depolarization of adult DRG neurons *in vitro* is a Na^+-dependent effect and may be mediated by activation of protein kinase C. Although it is clear that such depolarization will contribute to BK-induced excitation, there are other important factors that normally control the excitability of these neurons and that must be considered. For example, it has been shown that the excitability of some sensory neurons is regulated by at least two Ca^{2+}-activated K^+ conductances (fast and slow) (25, 26). In some cells, the slow $I_{K(Ca)}$ appears to play a particularly important role. Weinreich (4) has shown that BK is capable of inhibiting this slow $I_{K(Ca)}$. Weinreich and colleagues (4, 27) have proposed that this occurs via release of arachidonic acid, the generation of prostaglandin E_2, and subsequent stimulation of neuronal cAMP production. Our results suggest a similar effect of BK, although the mechanism is somewhat different. Thus, inhibition of the depolarization-induced Ca^{2+} influx by BK would also lead to a reduction in the $I_{K(Ca)}$. It is possible that this effect is mediated by a BK-induced activation of phospholipase A_2, although our studies have not investigated this point. One complicating issue that must be considered is that DRG cell cultures are clearly heterogeneous by several criteria, e.g., morphological neurochemical, and electrophysiological (9, 11, 12). It is clear even at this point that BK does not produce all of its diverse molecular effects in every cell. For example, in the present studies BK inhibited the I_{Ca} in 65% of cells but mobilized intracellular Ca^{2+} stores in only 20% of cells. From these and other observations reported here, it is clear that the BK-induced block of the I_{Ca} is not secondary to a BK-induced increase in $[Ca^{2+}]_i$ but is a separate GTP-binding protein-mediated event (5).

It should be noted that BK is only one of a number of agents that block voltage-sensitive Ca^{2+} channels in DRG neurons. Other agents in this category include NPY (28), GABA-B agonists (29), α_2-noradrenergic agonists (30), and opioids (31). In all these cases the effect of such agents *in situ* is to inhibit synaptic transmission from sensory afferent fibers in the spinal

cord (1, 28, 32, 33). This may appear anomalous, in view of the suggestion made above that the BK-induced inhibition of Ca^{2+} channels and $[Ca^{2+}]_i$ transients in DRG cells may contribute to the BK-induced excitation of these neurons and increased synaptic transmission. However, a solution to this apparent anomaly is evident from a consideration of the site of action of these various agents. Normally, the different inhibitory neurotransmitters mentioned have access to presynaptic sites of action within the spinal cord (1). Inhibition of Ca^{2+} channels at these sites will block the depolarization-induced $[Ca^{2+}]_i$ transient in the nerve terminal and result in a reduced neurotransmitter release. BK, on the other hand, does not have access to such presynaptic receptors in the spinal cord, because it exists predominantly in the periphery. BK is produced in response to injury at peripheral sites and does not cross the blood/brain barrier and enter the spinal cord. The action of BK on the peripheral terminals of sensory neurons would have the following effect. Inhibition of the depolarization-induced rise in $[Ca^{2+}]_i$ would reduce the normal inhibitory effect of $I_{K(Ca)}$. In addition, BK-induced depolarization would help to trigger the initiation of action potentials. The result is that increased numbers of spikes would propagate into the spinal cord and synaptic transmission would be increased. Thus, although BK and opiates, for example, both inhibit Ca^{2+} channels in sensory neurons, they produce precisely the opposite effects under normal conditions because they act at quite different points. Moreover, BK also has the ability to depolarize these neurons, which the other inhibitory substances alluded to do not. One prediction of this model is that, if BK was actually infused into the spinal cord and would, therefore, have access to presynaptic receptors, it might actually appear to be inhibitory. This is in fact exactly what happens (34, 35).

Although, as discussed above, BK does not normally produce presynaptic inhibition in DRG neurons *in vivo*, the way in which it modulates the depolarization-induced $[Ca^{2+}]_i$ transient does have important implications for those agents, such as opiates, NPY, α_2-adrenergic agonists, and GABA-B agonists, that do. As we demonstrate, the $[Ca^{2+}]_i$ transients in these cells produced by voltage steps or action potentials tend to an asymptote with application of longer voltage steps or spike trains (see also Ref. 36). The result is that the precise effect of BK on the $[Ca^{2+}]_i$ transient depends on the activation state of the cell. When the cell is strongly activated, the effect of BK on the amplitude of the $[Ca^{2+}]_i$ transient may be small or even absent. Presynaptic modulation of neurotransmitter release can probably be produced by a variety of mechanisms, including activation of GABA-A receptor-linked Cl^- channels. However, activation of some inhibitory presynaptic receptors (e.g., NPY, α_2-adrenergic, GABA-B, and opioid) seems to be linked to the inhibition of neuronal Ca^{2+} channels, as discussed above, and also the activation of K^+ conductances (37–39). In these instances, the inhibitory effects of neurotransmitters or drugs on synaptic transmission can inevitably be overcome by increasing the activation state of the cell (37–43). It has, in fact, been suggested that this is due to the "saturation of the $[Ca^{2+}]_i$ receptor" at high activation rates (40). Clearly, the results of our studies lend support to such a mechanism.

References

1. Yaksh, T. L., and D. L. Hammond. Peripheral and central substrates involved in the rostrad transmission of nociceptive information. *Pain* **13**:1–85 (1982).
2. Armstrong, D. Pain. *Handb. Exp. Pharmacol.* **25**:434–481 (1970).
3. Miller, R. J. Bradykinin highlights the role of phospholipid metabolism in the control of nerve excitability. *Trends Neurosci.* **10**:226–228 (1987).
4. Weinreich, D. Bradykinin inhibits a slow spike afterhyperpolarization in visceral sensory neurons. *Eur. J. Pharmacol.* **132**:61–63 (1986).
5. Ewald, D. A., P. C. Sternweis, I.-H. Pang, and R. J. Miller. Differential G-protein mediated coupling of neurotransmitter receptors to Ca^{2+} channels in rat dorsal root ganglion neurons *in vitro*. *Neuron* **3**:1185–1193 (1989).
6. Burgess, G. M., I. Mullaney, M. McNeill, P. M. Dunn, and H. P. Rang. An investigation of the second messengers involved in the mechanism of action of bradykinin in sensory neurones in culture. *J. Neurosci.* **9**:3314–3325 (1989).
7. Baccaglini, P. T., and P. G. Hogan. Some rat sensory neurones in culture express characteristics of differentiated pain cells. *Proc. Natl. Acad. Sci. USA* **80**:594–598 (1983).
8. Rang, H. P., and M. Ritchie. Activation of protein kinase C causes a depolarization of the rat vagus nerve associated with increased sodium conductance. *J. Physiol. (Lond.)* **391**:78P (1987).
9. Harper, A. A., and S. N. Lawson. Electrical properties of rat dorsal root ganglion neurons with different peripheral nerve conduction velocities. *J. Physiol. (Lond.)* **359**:47–63 (1985).
10. Sommer, E. W., J. Kazimierczak, and B. Droz. Neuronal subpopulations in the dorsal root ganglion of the mouse as characterized by combination of ultrastructural and cytochemical features. *Brain Res.* **346**:310–326 (1985).
11. Jessell, T. M., and J. Dodd. Structure and expression of differentiation antigens on functional subclasses of primary sensory neurons. *Philos. Trans. R. Soc. Lond. B. Biol. Sci.* **108**:271–281 (1985).
12. Schoenen, J., P. Delree, P. Leprince, and G. Moonen. Neurotransmitter phenotype plasticity in cultured dissociated adult rat dorsal root ganglia: an immunocytochemical study. *J. Neurosci. Res.* **22**:473–487 (1989).
13. Thayer, S. A., M. Sturek, and R. J. Miller. Measurement of neuronal Ca^{2+} transients using simultaneous microfluorimetry and electrophysiology. *Pflugers. Arch.* **412**:216–223 (1988).
14. Grynkiewicz, G., M. Poenie, and R. Y. Tsien. A new generation of Ca^{2+} indicators with greatly improved fluorescence properties. *J. Biol. Chem.* **260**:3440–3450 (1985).
15. Fabatio, A., and F. Fabatio. Calculator programs for computing the composition of the solutions containing multiple metals and ligands used for experiments in skinned muscle cells. *J. Physiol. (Paris)* **75**:463–505 (1979).
16. Glaum, S. R., J. A. Holzwarth, and R. J. Miller. Glutamate receptors activate Ca^{2+} mobilization and Ca^{2+} influx into astrocytes. *Proc. Natl. Acad. Sci. USA*, **87**:3454–3458 (1990).
17. Thayer, S. A., T. M. Perney, and R. J. Miller. Regulation of calcium homeostas in sensory neurons by bradykinin. *J. Neurosci.* **8**:4089–4097 (1988).
18. Hamill, O., A. Marty, E. Neher, B. Sakmann, and F. Sigworth. Improved patch clamp technique for high resolution current recording from cells and cell free membrane patches. *Pflugers Arch.* **391**:85–100 (1981).
19. Perney, T. M., and R. J. Miller. Two different G-proteins mediate neuropeptide Y and bradykinin stimulated phospholipid breakdown in cultured rat sensory neurons. *J. Biol. Chem.* **264**:7317–7327 (1989).
20. Szolcsanyi, J. Capsaicin: a new hot pharmacological tool. *Trends Neurosci.* **4**:495–497 (1984).
21. Bleakman, D., J. R. Brorson, and R. J. Miller. The effect of capsaicin on voltage gated calcium currents and calcium signals in cultured dorsal root ganglion cells. *Br. J. Pharmacol.*, **101**:423–431 (1990).
22. Thayer, S. A., and R. J. Miller. Regulation of the intracellular free calcium concentration in single rat dorsal root ganglion neurones *in vitro*. *J. Physiol. (Lond.)* **425**:85–115 (1990).
23. Ahmed, Z., and J. A. Connor. Calcium regulation by and buffer capacity of molluscan neurons during calcium transients. *Cell Calcium* **9**:57–69 (1988).
24. Benham, C. D. ATP activated channel gated calcium entry in single smooth muscle cells dissociated from rabbit ear artery. *J. Physiol. (Lond.)* **419**:689–701 (1989).
25. Weinreich, D., and W. F. Wonderlin. Inhibition of calcium-dependent spike afterhyperpolarization increases excitability of rabbit visceral sensory neurons. *J. Physiol. (Lond.)* **394**:415–427 (1987).
26. Fowler, J. C., R. Greene, and D. Weinreich. Two calcium sensitive spike afterhyperpolarizations in visceral sensory neurons of the rabbit. *J. Physiol. (Lond.)* **365**:59–75 (1985).
27. Fowler, J. C., W. F. Wonderlin, and D. Weinreich. Prostaglandins block a Ca^{2+} dependent slow spike afterhyperpolarization independent of effects on Ca^{2+} influx in visceral afferent neurons. *Brain Res.* **345**:345–349 (1985).
28. Walker, M. W., D. E. Ewald, T. M. Perney, and R. J. Miller. Neuropeptide Y modulates neurotransmitter release and Ca^{2+} currents in rat sensory neurons. *J. Neurosci.* **8**:2438–2446 (1988).
29. Dolphin, A. C., and R. H. Scott. Calcium currents and their inhibition by (−)-baclofen in rat sensory neurons: modulation by guanine nucleotides. *J. Physiol. (Lond.)* **386**:1–17 (1987).
30. Dunlap, K., and G. D. Fischbach. Neurotransmitters decrease the calcium conductance activated by depolarizing embryonic chick sensory neurons. *J. Physiol. (Lond.)* **317**:519–535 (1981).
31. MacDonald, R., and M. A. Werz. Dynorphin A decreases voltage dependent calcium conductance of mouse dorsal root ganglion neurons. *J. Physiol. (Lond.)* **377**:237–249 (1986).
32. Holz, G. G., R. M. Kream, A. Spiegel, and K. Dunlap. G-proteins couple α-

adrenergic and GABA-B receptors to inhibition of peptide secretion from peripheral sensory neurons. *J. Neurosci.* **9**:657–666 (1989).
33. Yaksh, T. L., T. M. Jessell, R. Gamse, A. W. Mudge, and S. E. Leeman. Intrathecal morphine inhibits substance P from mammalian spinal cord *in vivo*. *Nature* (*Lond.*) **286**:155–156 (1980).
34. Laneuville, O., and R. Couture. Bradykinin analogue blocks bradykinin induced inhibition of a spinal nociceptive reflex in the rat. *Eur. J. Pharmacol.* **137**:281–290 (1987).
35. Laneuville, O., T. A. Reader, and R. Couture. Intrathecal bradykinin acts presynaptically on spinal noradrenergic terminals to produce antinociception in the rat. *Eur. J. Pharmacol.* **159**:273–283 (1989).
36. Zucker, R. S. Short term synaptic plasticity. *Annu. Rev. Neurosci.* **12**:13–31 (1980).
37. Nicoll, R. A. The coupling of neurotransmitter receptors to ion channels in the brain. *Science* (*Washington D. C.*) **241**:545–555 (1988).
38. Belardetti, F., and S. A. Siegelbaum. Up and down modulation of single K^+ channel function by distinct second messengers. *Trends Neurosci.* **11**:232–238 (1988).
39. Van Dongen, A. M. J., J. Codina, J. Obate, R. Mattera, R. Joho, L. Birnbaumer, and A. M. Brown. Newly identified brain potassium channels gated by the guanine nucleotide binding protein G_o. *Science* (*Washington D. C.*) **242**:1433–1437 (1988).
40. Starke, K. Presynaptic α-autoreceptors. *Rev. Physiol. Biochem. Pharmacol.* **107**:74–146 (1987).
41. Budai, D., and S. P. Duckles. Influence of stimulation train length on the opioid induced inhibition of norepinephrine release in the rabbit ear artery. *J. Pharmacol. Exp. Ther.* **247**:839–843 (1988).
42. Stretton, C. D., and P. J. Barnes. Modulation of cholinegic neurotransmission in guinea pig trachea by neuropeptide Y. *Br. J. Pharmacol.* **13**:672–678 (1988).
43. Grundemar, L., E. Widmark, B. Waldeck, and R. Hakanson. Neuropeptide Y: Prejunctional inhibition of vagally induced contractions in the guinea-pig trachea. *Regul. Peptides* **23**:309–313 (1988).

Send reprint requests to: Dr. Richard J. Miller, Department of Pharmacological and Physiological Sciences, University of Chicago, 947 East 58th Street, Chicago, IL 60637.